AMERICAN SOCIETY FOR MICROBIOLOGY | mSystems®

RESEARCH ARTICLE
Applied and Environmental Science

Contrasting Pathways for Anaerobic Methane Oxidation in Gulf of Mexico Cold Seep Sediments

Adrien Vigneron,[a,b] Eric B. Alsop,[b,c] Perrine Cruaud,[d] Gwenaelle Philibert,[b] Benjamin King,[b] Leslie Baksmaty,[b] David Lavallee,[b] Bartholomeus P. Lomans,[e] Emiley Eloe-Fadrosh,[c] Nikos C. Kyrpides,[c] Ian M. Head,[a] Nicolas Tsesmetzis[a,b]

[a]School of Natural and Environmental Sciences, Newcastle University, Newcastle Upon Tyne, United Kingdom
[b]Shell International Exploration and Production Inc., Houston, Texas, USA
[c]DOE Joint Genome Institute, Walnut Creek, California, USA
[d]Departement de Biochimie, de Microbiologie, et de Bio-Informatique, Faculté des Sciences et de Génie, Université Laval, Quebec City, Quebec, Canada
[e]Shell Global Solutions International B.V., Rijswijk, Netherlands

ABSTRACT Gulf of Mexico sediments harbor numerous hydrocarbon seeps associated with high sedimentation rates and thermal maturation of organic matter. These ecosystems host abundant and diverse microbial communities that directly or indirectly metabolize components of the emitted fluid. To investigate microbial function and activities in these ecosystems, metabolic potential (metagenomic) and gene expression (metatranscriptomic) analyses of two cold seep areas of the Gulf of Mexico were carried out. Seeps emitting biogenic methane harbored microbial communities dominated by archaeal anaerobic methane oxidizers of phylogenetic group 1 (ANME-1), whereas seeps producing fluids containing a complex mixture of thermogenic hydrocarbons were dominated by ANME-2 lineages. Metatranscriptome measurements in both communities indicated high levels of expression of genes for methane metabolism despite their distinct microbial communities and hydrocarbon composition. In contrast, the transcription level of sulfur cycle genes was quite different. In the thermogenic seep community, high levels of transcripts indicative of syntrophic anaerobic oxidation of methane (AOM) coupled to sulfate reduction were detected. This syntrophic partnership between the dominant ANME-2 and sulfate reducers potentially involves direct electron transfer through multiheme cytochromes. In the biogenic methane seep, genes from an ANME-1 lineage that are potentially involved in polysulfide reduction were highly expressed, suggesting a novel bacterium-independent anaerobic methane oxidation pathway coupled to polysulfide reduction. The observed divergence in AOM activities provides a new model for bacterium-independent AOM and emphasizes the variation that exists in AOM pathways between different ANME lineages.

IMPORTANCE Cold seep sediments are complex and widespread marine ecosystems emitting large amounts of methane, a potent greenhouse gas, and other hydrocarbons. Within these sediments, microbial communities play crucial roles in production and degradation of hydrocarbons, modulating oil and gas emissions to seawater. Despite this ecological importance, our understanding of microbial functions and methane oxidation pathways in cold seep ecosystems is poor. Based on gene expression profiling of environmental seep sediment samples, the present work showed that (i) the composition of the emitted fluids shapes the microbial community in general and the anaerobic methanotroph community specifically and (ii) AOM by ANME-2 in this seep may be coupled to sulfate reduction by *Deltaproteobacteria* by electron transfer through multiheme cytochromes, whereas AOM by ANME-1 lineages in this seep may involve a different, bacterium-independent pathway, coupling methane oxidation to elemental sulfur/polysulfide reduction.

Citation Vigneron A, Alsop EB, Cruaud P, Philibert G, King B, Baksmaty L, Lavallee D, Lomans BP, Eloe-Fadrosh E, Kyrpides NC, Head IM, Tsesmetzis N. 2019. Contrasting pathways for anaerobic methane oxidation in Gulf of Mexico cold seep sediments. mSystems 4:e00091-18. https://doi.org/10.1128/mSystems.00091-18.

Editor Steven J. Hallam, University of British Columbia

Address correspondence to Adrien Vigneron, avignero@gmail.com.

Different AOM pathways in cold seep sediments with potential polysulfide reduction by ANME-1 lineage

Received 8 June 2018
Accepted 4 February 2019
Published 26 February 2019

KEYWORDS AOM, metagenomic, metatranscriptomic, methane, polysulfide

Methane seeps are widespread in marine environments, particularly in continental margins where deeply buried organic matter is progressively transformed to hydrocarbons (1). Large and diverse chemosynthetic communities flourish in these environments, and surface sediments are often colonized by conspicuous macrofaunal assemblages (e.g., bivalves, tube worms) or microbial mats, depending on the emitted fluids (2, 3). The surface communities are fueled by hydrocarbons in the seeping fluids and metabolic products from the sedimentary microbial communities. Numerous microbial lineages occur in these environments. Many of these remain uncultured, and their potential functions remain poorly characterized (4). Microbial community analyses (2, 3, 5) and activity measurements (6, 7) indicated that community composition and metabolic activities depend on fluid flow rate and hydrocarbon composition. Nevertheless, anaerobic methanotrophs are almost ubiquitous in these environments (8). They frequently represent the predominant microorganisms in the sulfate- and methane-rich sediment layers of marine seep ecosystems, consuming up to 90% of the methane from the seep in the absence of oxygen (9). Anaerobic oxidation of methane (AOM) in marine methane seep sediments was first discovered associated with syntrophic aggregates of archaeal *an*aerobic *me*thanotrophs (ANME) and sulfate-reducing bacteria (SRB) from the *Deltaproteobacteria*, where methane oxidation is coupled to sulfate reduction (10). Exploration of seep sediments around the world has led to the identification of various ANME lineages, including ANME-1a, -1b, -2ab, -2c, and -3 (3, 9, 11), as well as lineages that seem to be geographically restricted (ANME-1 Guaymas groups [12], Aarhus Bay M5 ANME-1 [13]). Concomitantly, deltaproteobacterial members of AOM consortia, including the SEEP SRB1a cluster from the *Desulfosarcina/Desulfococcus* group (14, 15), some *Desulfobulbus* lineages (16, 17), SEEP SRB2 from hydrothermal systems (18, 19), and "*Candidatus* Desulfofervidus"/hot seep 1 (20, 21), have been discovered. Other lineages, such as members of the *Verrucomicrobia*, have also been suspected to play a role in AOM consortia (22). While some variation in metabolism seems to occur within ANME lineages (23), genomic (24) and proteomic (25) studies indicated that all anaerobic methanotrophs oxidize methane to CO_2 using a reverse-methanogenesis pathway. However, debate remains about the mechanisms whereby methane oxidation is coupled to respiratory pathways, and this seems to be dependent on the specific organisms involved (23). For example, the role of each of the partners and how archaeal and bacterial metabolism in AOM consortia are coupled remain a matter of discussion (26). Initially, AOM was thought to be carried out by archaeal ANME with hydrogen, electrons, or low-molecular-weight organic acids (formate or acetate) providing the energy source for the syntrophic sulfate reducing bacterial partners (9, 10). Other data suggested that ANME-2 could reduce sulfate to polysulfide and elemental sulfur (S^0) via an as-yet-uncharacterized pathway (27). In this process, which remains to be supported by the identification of the genes involved, S^0 possibly in the form of polysulfide is the proposed intermediate electron carrier that links the metabolism of the ANME archaea to sulfur-disproportioning *Deltaproteobacteria* (27). Alternatively, conductive pili (nanowires) and multiheme cytochromes, analogous to the outer membrane cytochromes involved in extracellular electron transfer in, e.g., *Geobacter* spp., were reported in ANME-2/SEEP SRB1 (28) and ANME-1/hot seep 1 aggregates isolated from Guaymas Basin hydrothermal sediments (29). Analysis of genomic bins, gene expression, and ultrastructure of meso- and thermophilic AOM consortia revealed that genes encoding putative electrically conductive proteins were highly expressed in AOM consortia (30). Direct electron transfer through extracellular conductive proteins may therefore be a key mechanism coupling the metabolism of ANME and sulfate-reducing bacteria in some AOM assemblages (28, 29, 31). Nitrate can also be reduced by specific lineages of ANME, like "*Candidatus* Methanoperedens nitroreducens" and the ANME-2d that have and express a nitrate reductase gene (*narG*) directly accepting electrons from AOM (11, 32). Metal ions (33–35) and extracellular

quinones (36) can also be used as electron acceptors by ANME-2 for AOM. Interestingly, the use of extracellular quinones as electron acceptors for AOM can decouple this process from bacterial activity (36). Potential independence of AOM from bacterial involvement has also been inferred from fluorescence *in situ* hybridization (FISH) analysis of aggregates of ANME-1, -2a, and -3, which showed no detectable bacterial partner (17, 37, 38), questioning obligate syntrophic models of ANME metabolism in methane seep environments. Gene expression profiling has been carried out on mesophilic and thermophilic AOM consortia that have been maintained in the laboratory for over 2 years (30). This has revealed extracellular electron exchanges between ANME and sulfate-reducing bacteria. Likewise, genetic composition and expression of a single ANME-2a aggregate obtained after 1 year of incubation in a high-pressure bioreactor and a nitrate-reducing freshwater ANME-2d from a bioreactor have been explored, revealing ANME-2 lineage metabolic specificities. Metaproteomic analysis of ANME-rich microcosms has also been carried out, depicting differences in expression of proteins involved in the methane metabolism between ANME variants. Together, these results highlighted a strong variability or flexibility in ANME metabolism. However, it is uncertain how these results can be extrapolated to *in situ* activities and how AOM consortia function in low-temperature seep environments with different and fluctuating seepage composition and regimens.

To better understand the different microbial processes in methane seep sediments in relation to fluid composition, the metabolic potential (metagenomic) and gene expression (metatranscriptomic) patterns of two contrasting Gulf of Mexico seep sediments were investigated, providing a snapshot of potential activities of the complex ANME-dominated microbial communities. Given the apparent metabolic versatility of ANME archaea, we hypothesized that hydrocarbon seeps with different fluid compositions harbor different microbial communities catalyzing AOM and that these may exhibit different routes of methane oxidation.

RESULTS

Geochemical characteristics of the seep sediments. Sediment push cores (15 cm long) from two different cold seep sites from the Mississippi Canyon of the Gulf of Mexico were analyzed (Fig. 1): (i) a cold seep area (push core 1 [PC1]) covered by orange microbial mats and (ii) a slowly emitting gas seep (PC10) showing sporadic bubble emission surrounded by scattered white mat-like traces at the sediment surface. PC1 sediments, which exhibited intense gas bubbling at the seafloor, harbored high hydrocarbon concentrations, with up to 85.45 μM methane, 39 μM ethane, 21 μM propane, and 61.5 μM butane (Fig. 1). The presence of these alkanes as well as the δ^{13}C of methane (–54.6 ‰) suggested a mixed thermogenic/biogenic source with a predominantly thermogenic origin of the hydrocarbon fluid. In contrast, PC10 sediments, which exhibited limited bubbling at the seafloor, had lower hydrocarbon concentrations, with up to 2.55 μM methane within the sampled sediment horizons. The δ^{13}C of methane was –68.7‰, and no other hydrocarbons were detected, suggesting a different seep origin (39). PC1 sediment exhibited a low sulfate concentration (1.71 mM) relative to the seawater concentration and the absence of detectable sulfite. At a depth of 3 to 4 cm below the sea floor (cmbsf), PC10 contained 7.88 mM sulfate and 0.12 mM sulfite, whereas the deeper sediment layer (10 to 12 cmbsf) contained 12.93 mM sulfate and 0.13 mM sulfite (Fig. 1).

Microbial community composition. Microbial community composition under the different seepage compositions and regimens was determined by analyzing the 16S rRNA genes and transcripts extracted from metagenomic and metatranscriptomic sequencing data (Fig. 2). The DNA-based metagenomes had relatively similar microbial community compositions (Bray-Curtis similarity, 60.7% and 60.1% between PC1 3- to 4-cmbsf and PC10 3- to 4-cmbsf and 10- to 12-cmbsf sediment samples, respectively, and 74% between PC10 3- to 4-cmbsf and PC10 10- to 12-cmbsf sediment samples). Based on the number of 16S rRNA genes recovered from metagenomes, the bacteria represented on average 74% $\pm$ 7% of the total microbial community and was domi-

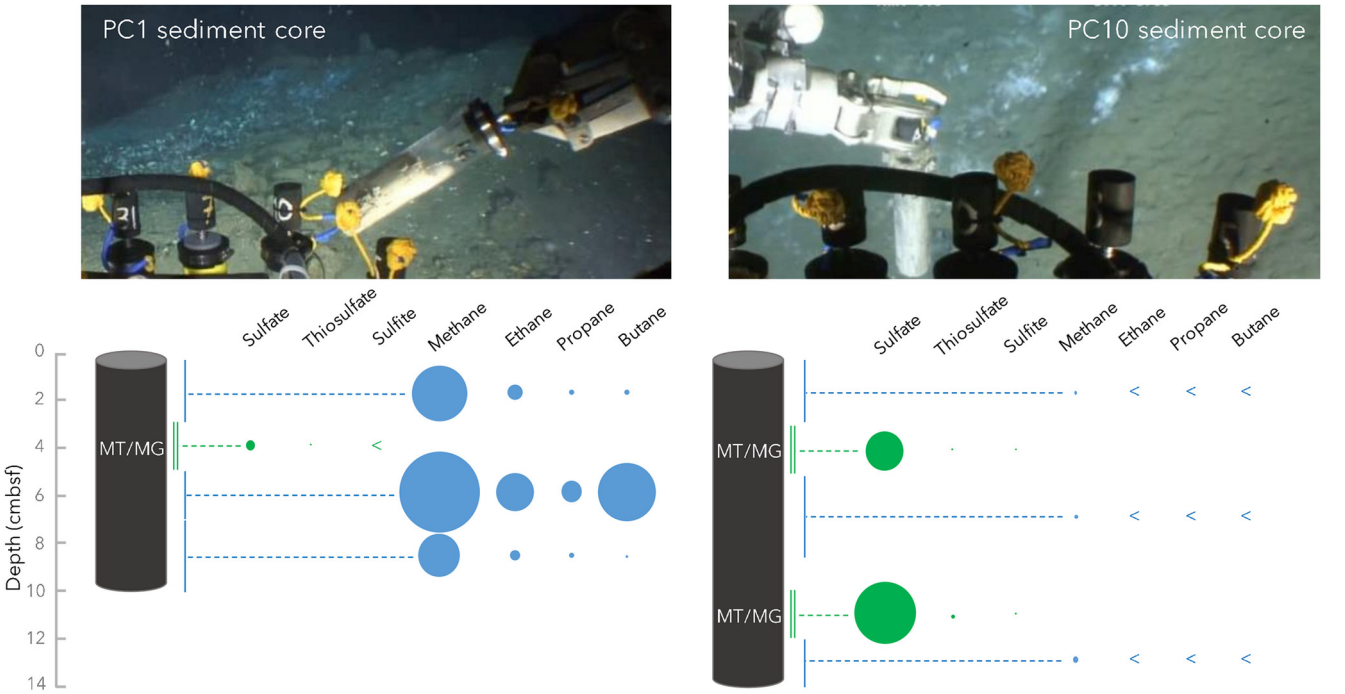

Samples	Nitrate (mM)	Sulfate (mM)	Thiosulfate (mM)	Sulfite (mM)	Methane (μM)	Ethane (μM)	Propane (μM)	Butane (μM)	δC13-CH_4 (‰)	δC13-C2 (‰)	δC13-C3 (‰)	δC13-C4 (‰)
PC1 0-3 cmbsf	-	-	-	-	59.05	15.3	4.5	5.3	-50.6	-	-	-
PC1 3-4 cmbsf	5	1.71	0.22	ND	-	-	-	-	-	-	-	-
PC1 5-7 cmbsf	-	-	-	-	85.45	39.3	21.8	61.5	-52.8	-28.7	-26.3	-23.7
PC1 7-10 cmbsf	-	-	-	-	43.92	11.2	5.9	2.7	-54.6	-	-	-
PC10 0-3 cmbsf	-	-	-	-	0.04	ND	ND	ND	ND	-	-	-
PC10 3-4 cmbsf	ND	7.88	0.11	0.12	-	-	-	-	-	-	-	-
PC10 5-10 cmbsf	-	-	-	-	0.06	ND	ND	ND	ND	-	-	-
PC10 10-12 cmbsf	ND	12.93	0.61	0.13	-	-	-	-	-	-	-	-
PC10 12-15 cmbsf	-	-	-	-	2.55	ND	ND	ND	-68.7	-	-	-

FIG 1 Pictures of the study sites with geochemical characterization of sediment samples. ND, not detected; -, not available for analysis; MT/MG, metatranscriptomes/metagenomes.

nated by members of the *Chloroflexi* (13% ± 3%), various *Deltaproteobacteria* (13% ± 2%), *Epsilonproteobacteria* (4% ± 2%), candidate division JS1 (*Atribacteria*, 4% ± 1%), OD1 (3% ± 1%), and *Bacteroidetes* (6% ± 4%) (Fig. 2). The archaeal community (24% ± 7% of the microbial 16S rRNA gene reads) was dominated by anaerobic methanotrophs ANME-1b (9% ± 3%), marine benthic group D (4% ± 1%), and *Thermoplasmata* (4 ± 0.8%) (Fig. 2). Notwithstanding that in some cases cells can maintain high levels of ribosomes, even when not metabolically active (40, 41), metatranscriptomic data were used as a proxy for the detection of metabolically active populations. The microbial community composition obtained from metatranscriptomic data presented a different profile from that of metagenomic data (Fig. 2). On the basis of sequences extracted from the metatranscriptome, 16S rRNA sequences from archaea represented 45% of the reads in sediment from 3 to 4 cmbsf at both sites PC1 and PC10 and up to 64% of the 16S rRNA reads from 10 to 12 cmbsf at site PC10. ANME-1b organisms were the predominantly active archaea in PC10 sediments (32% ± 11% of rRNA reads), whereas ANME-2 organisms were the most active archaea in the PC1 sample (30% of rRNA reads) (Fig. 2). The metabolically active fraction of the bacterial community was dominated by deltaproteobacterial lineages, with the SEEP SRB2 group proving to be the most active bacteria in PC10 sediment samples and the SEEP SRB1 group and *Desulfobacteraceae* being the most active bacteria in PC1 sediments (Fig. 2).

Methane-cycling community composition. Methane-producing and -oxidizing archaea were also identified by analysis of the genes encoding the alpha subunit of the

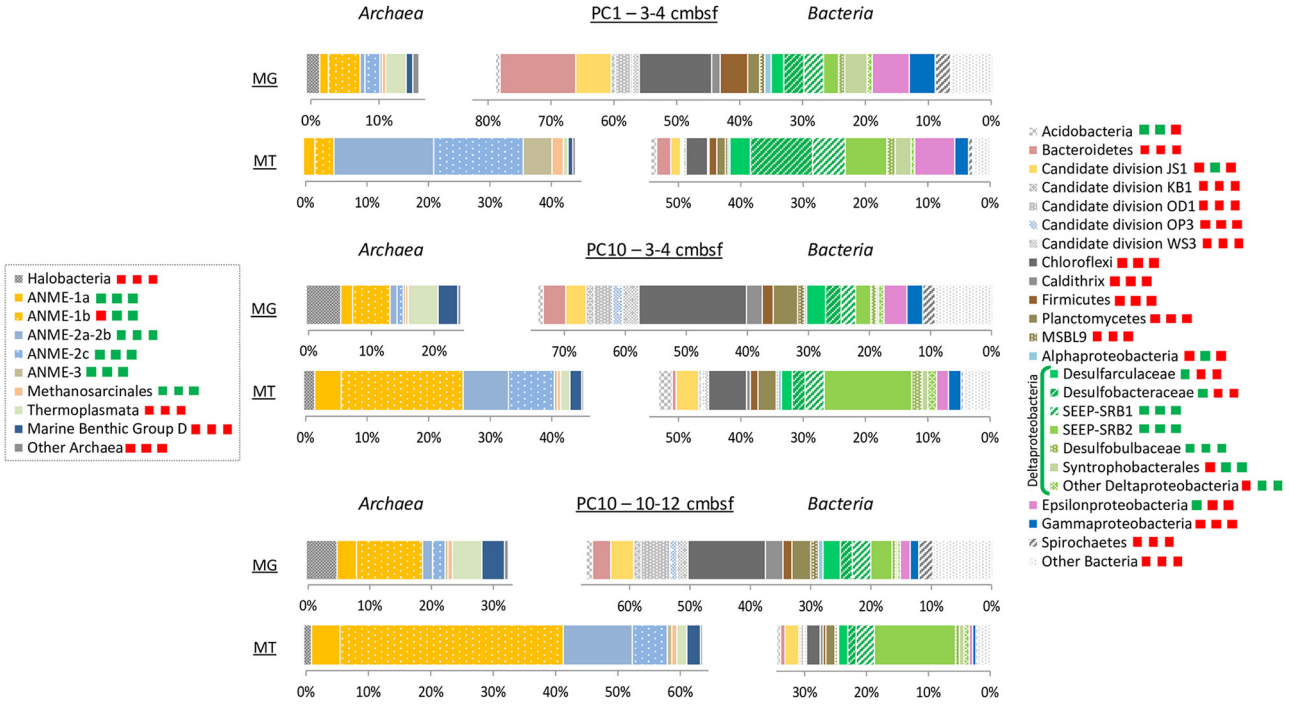

FIG 2 Taxonomic affiliation of 16S rRNA genes (MG) and transcripts (MT) in PC1 and PC10 sediment samples. MG, metagenomes; MT, metatranscriptomes. Shades of green represent *Deltaproteobacteria* families. Phyla representing less than 1% of the reads are gathered under "Other Bacteria." Archaea and bacteria are spaced to highlight the relative proportion of each domain but represented together 100% of the detected 16S rRNA genes and transcripts. Colored squares in the keys represent the ratios of 16S rRNA transcripts to genes for each lineage in PC1 at 3 to 4 cmbsf, in PC10 at 3 to 4 cmbsf, and in PC10 at 10 to 12 cmbsf (in that order), with an MT/MG ratio of >1 in green and an MT/MG of <1 in red.

methyl-coenzyme M reductase (*mcrA*) and their corresponding transcripts (Fig. 3a; see also Fig. S1 in the supplemental material). Taxonomic affiliation of the *mcrA* reads using an *mcrA*-specific gene database (42) followed by phylogenetic tree reconstruction indicated that both anaerobic methanotrophs and methanogens were present in the

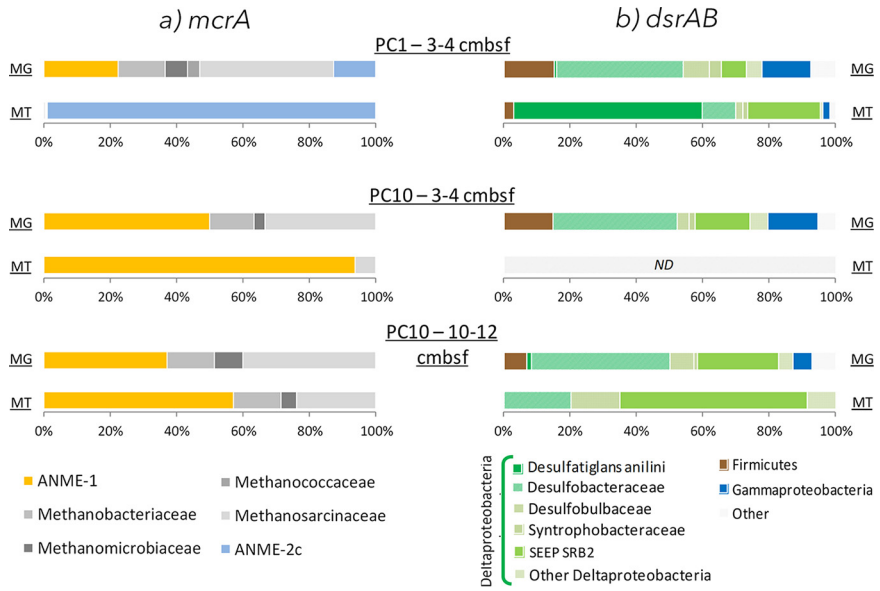

FIG 3 Taxonomic affiliation of *mcrA* (a) and *dsrAB* (b) metagenomes (MG) and metatranscriptomes (MT) in PC1 and PC10 sediment samples. Shades of green represent *Deltaproteobacteria* families. ANME-1 subgroup affiliation was not possible using BLAST but was determined using a phylogenetic tree with reconstructed full-length *mcrA* genes and transcripts (Fig. S1).

sediment samples (Fig. 3a). In PC10 sediment, ANME-1b organisms were the only anaerobic methanotrophs identified, as well as the most active methane-cycle lineage (which consisted of up to 97% of the *mcrA* transcripts in PC10 3- to 4-cmbsf samples) (Fig. 3a; Fig. S1). In contrast, in PC1 sediment samples, although *mcrA* gene sequences were affiliated to ANME-1, ANME-2c, and methanogenic lineages, 98% of the *mcrA* transcripts were related to the ANME-2c lineage (Fig. 3a). Few reads of aerobic methane oxidation genes (*pmoA*, *mmoA*) were detected in PC1 and PC10 3- to 4-cmbsf samples (their read numbers were 25 times less than the *mcrA* read numbers in the same samples), and no transcripts of *pmoA* nor *mmoA* were detected in the samples.

Sulfate reducer community composition. Sequences of the genes and transcripts for dissimilatory sulfite reductase (*dsrAB*) were analyzed using a *dsrAB* database (43) and phylogenetic analysis to identify sulfate-reducing bacteria (Fig. 3b; Fig. S1). Based on the proportion of *dsrAB* reads from metagenomic data, sulfate-reducing bacterial community composition in all samples was dominated by members of the *Desulfobacteraceae*, *Desulfobulbaceae*, *Firmicutes*, and an environmental cluster of cold seep clones, potentially corresponding to the SEEP SRB2 group identified by 16S rRNA analysis (Fig. 3b; Fig. S1). However, metatranscriptome analysis revealed that the most abundant SRB were potentially not active as sulfate reducers. Indeed, no *dsrAB* transcripts from over 130,000 transcripts of functional genes were detected in sediment samples taken from 3 to 4 cmbsf at site PC10. Transcripts from *dsrAB* genes detected in sediments from 10 to 12 cmbsf at site PC10 were affiliated mainly with *dsrAB* genes from SEEP SRB2 and, to a lesser degree, *Desulfobacteraceae*, though metagenome analysis inferred that the *Desulfobacteraceae* were more prevalent. Metatranscriptome-derived *dsrAB* sequences from PC1 sediments were dominated by reads from the *Desulfatiglans anili* lineage, SEEP SRB2, and SEEP SRB1 (*Desulfobacteraceae*), which were present at much lower frequency in the metagenome data (Fig. 3b; Fig. S1).

Gene expression in the microbial communities. A total of 8,092 different functional genes (KEGG orthologs [KO]) were identified in the metagenomes derived from the sediment samples. After rRNA removal and multiple normalizations to 130,000 reads of functional gene transcripts, 54.2% (4,385) of the genes detected in the metagenomes were shown to be expressed (more transcripts than the corresponding genes) in at least one sediment sample (Fig. S2). Although we cannot exclude the possibility that some of the short half-life mRNA molecules had been degraded or that gene expression could have been modified during the recovery of the cores, detected transcripts were consistent with potential cold seep activities. Overall metagenomic and metatranscriptomic analysis of the sediment samples indicated that genes potentially involved in methanogenesis or AOM (*fmdABCDE*, *ftr*, *mch*, *mtd*, *fae-hps*, *metF*, *cdhCDG*, *mtrABCDEGH*, *mcrABCG*) were strongly represented and expressed in all samples (on average, the $\log_2$ fold change [$\log_2$FC] was 1.1 ± 0.3) (Fig. 4; Fig. S2) and detected in the ANME-1-recruited reads (ANME-1-recruited reads formed a genomic bin with a completeness level at 82.55%, contamination level at 8.86%, and strain heterogeneity at 14.5%) (Fig. 4). Genes of the cytoplasmic Hdr1 (*hdrABC*) and Hdr2 (*mvhD frhB hdr*) complexes and *fqo* were also identified in metagenomic and metatranscriptomic data sets and in ANME-1-recruited reads (Fig. 4). Genes coding for Rnf and Ech hydrogenases were also detected in unassembled data but not recruited in the ANME-1 bin. Furthermore, no transcripts of *ech* and very low transcript levels of *rnf* were detected in the samples (on average, $\log_2\text{FC} = -1.8$). Based on the taxonomic affiliations of these genes and transcripts, most of the *rnf* sequences belonged to deltaproteobacterial lineages, whereas *ech* genes were associated with *Firmicutes* or *Epsilonproteobacteria*. Multiheme cytochrome *c* genes, involved in extracellular electron transfer, were also identified in all samples and in the ANME-1 reads. However, a positive transcription level (more transcripts than genes) was detected only in the PC1 sediment sample ($\log_2\text{FC} = 1.72$ in PC10) (Fig. 4). Genes for cytochrome *b* were present, but fewer transcripts than genes were detected in all samples ($\log_2\text{FC} = -1.2$), and *cytB* genes were not identified in ANME-1-recruited reads but were related to various

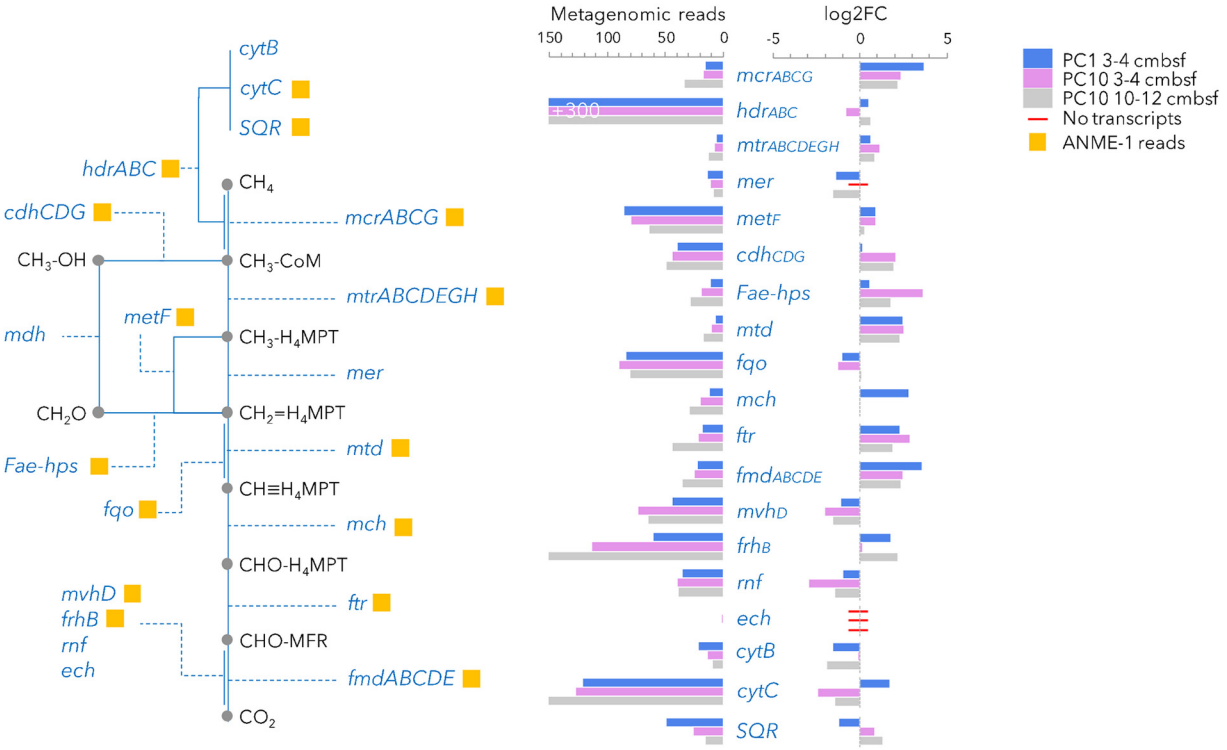

FIG 4 Schematic representation of the (reverse)-methanogenesis pathway. Numbers of metagenomic reads (after normalization) for each gene of the (reverse)-methanogenesis pathway and its gene expression level (log_2 fold change) detected in PC1 at 3 to 4 cmbsf (blue), in PC10 at 3 to 4 cmbsf (purple), and in PC10 at 10 to 12 cmbsf (gray) are shown. Red lines indicate that no transcripts were detected. Yellow squares indicate the presence of the gene in ANME-1-recruited reads. CoM, coenzyme M; H_4MPT, *N*5,*N*10-methylene-tetrahydromethanopterin; MFR, methanofuran.

proteobacterial lineages. Genes for nitrate (*narGH*) and nitrite (*nirB*) reduction pathways were investigated to explore a potential link between nitrogen cycling and AOM (11, 32). These genes as well as the potential for nitrogen fixation (*nifBDEFHK*) were detected in all samples (Fig. S3). However, metatranscriptomic data indicated that only genes for nitrogen fixation (*nifBDEFHK*, $log_2FC = 1.23 \pm 0.6$), affiliated mainly with ANME communities, were expressed in all samples, whereas no transcript or fewer transcripts than genes were detected for nitrate reduction genes that were affiliated with gammaproteobacterial lineages ($log_2FC = -4.7$ in sample PC1) (Fig. S3). Genes for sulfate (*sat*, *aprA*, *dsrAB*), thiosulfate (*TST*), elemental sulfur (*hydABCD*), and polysulfide (*psrAC* or *phsAC*) reduction as well as genes for sulfide oxidation (*sox*, sulfide:quinone oxidoreductase-like [SQR] gene) were detected in all sediment samples (Fig. 5). Sulfate reduction genes (*aprA* and *dsrAB*) were expressed (more transcripts than genes) in sediment sample PC1 ($log_2FC = 0.88$), whereas low levels of expression of these genes ($log_2FCs = 0.45$ and -0.75 for *dsrAB* and *aprA,* respectively) were detected in PC10 at 10 to 12 cmbsf, and no transcripts were detected in PC10 at 3 to 4 cmbsf. Thiosulfate/polysulfide reduction genes (*psrA* and *phsA*) were expressed in PC10 at 3 to 4 cmbsf ($log_2FC = 1.27$), with transcripts affiliated with the *Atribacteria* (candidate division JS1/OP9). Genes involved in elemental sulfur reduction and thiosulfate oxidation were not expressed or were expressed at very low levels in the samples. The SQR gene, affiliated mainly with ANME-1 (91% of the genes and transcripts were homologous to ANME-1-recruited sequences), was expressed in PC10 both at 3 to 4 cmbsf and at 10 to 12 cmbsf ($log_2FC = 1.08 \pm 0.3$). Genes and transcripts encoding an F420-dependent sulfite reductase (Fsr) affiliated with ANME communities were detected in all sediment samples but at highest relative abundance in PC10 at 3 to 4 and 10 to 12 cmbsf (2 and 4 times more genes and transcripts than in PC1 samples) (Fig. 5; Fig. S2). Genes and transcripts involved in assimilatory sulfate reduction (*cysNDCHIJ*) were also detected in all samples (Fig. 5) and were affiliated mainly with ANME communities, *Firmicutes*, and

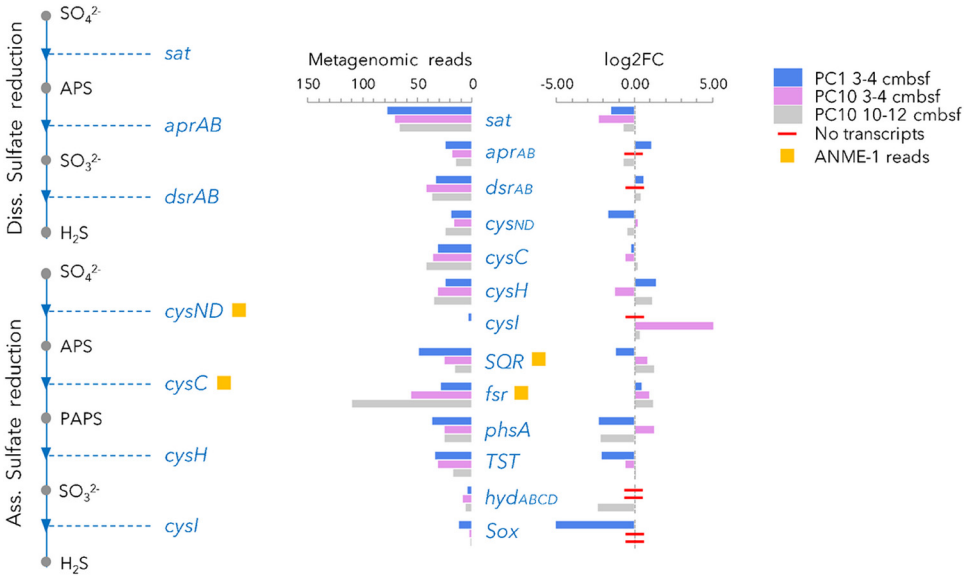

FIG 5 Schematic representations of the dissimilatory (Diss.) and assimilatory (Ass.) sulfate reduction pathways. Numbers of metagenomic reads (after normalization) for each gene of the sulfur cycle and its gene expression level (log_2 fold change) detected in PC1 at 3 to 4 cmbsf (blue), in PC10 at 3 to 4 cmbsf (purple), and in PC10 at 10 to 12 cmbsf (gray) are shown. Red lines indicate that no transcripts were detected. Yellow squares indicate the presence of the gene in ANME-1-recruited reads. APS, adenylyl sulfate; PAPS, 3′-phosphoadenylyl sulfate; *SQR*, sulfide-quinone oxidoreductase; *fsr*, F420-dependent sulfite reductase; *phsA*, thiosulfate/polysulfide reduction; *TST*, thiosulfate reduction; *hydABCD*, elemental sulfur reduction; *Sox*, thiosulfate/sulfur oxidation pathway.

Bacteroidetes. Additionally, genes involved in the anaerobic degradation of alkanes (*assA* or *bssA*, *bbsEF*) and aromatic hydrocarbons (*aliB*, *badADI*, *bnsE*, *nylB*) that were related to sequences from deltaproteobacterial lineages (*Desulfatiglans*, *Desulfobacteraceae*, and *Syntrophobacteraceae*) were identified in all samples (Fig. S3). The relative proportion of these genes was greater (2.7 times more reads) in the PC1 sediment sample than in the PC10 samples (2-fold more reads than in PC10 at 3 to 4 cmbsf and 3.4 times more than in PC10 at 10 to 12 cmbsf). However, fewer transcripts than genes were detected in all sediment samples, indicating that not all of the organisms carrying these genes expressed them at the time of sampling (Fig. S3).

DISCUSSION

Coupled metagenomics and metatranscriptomics provide useful perspectives on microbial activity and microbial responses to changing environmental conditions (44), revealing metabolic niches (45), metabolic pathways, and potential syntrophic interactions in complex microbial communities (46, 47). Despite extensive analysis of cold seep microbial communities (8, 9, 37, 48–50), there have been comparatively few reports of gene expression profiling of these environments, and these have been based largely on single-gene analyses (51) or enrichments (11, 25, 27–30, 38). Although the latter studies bring valuable insights into AOM consortia and ANME functioning, it remains unclear whether microbial activities in controlled microcosms (25) and sediment-free enrichments maintained for more than a year under laboratory conditions (30, 38) reflect *in situ* activities. Moreover, measuring rates of activity *in situ* and isotopic labeling are difficult to set up with remotely operated vehicles (ROVs) operating on the seafloor, and activity measurements are constrained to metatranscriptomic and proteomic analyses of sediment samples, presenting a snapshot of the *in situ* microbial activity. In this study, we combined metagenomic and metatranscriptomic sequencing to investigate the potentially active metabolic processes in two hydrocarbon seep locations in the Gulf of Mexico. Distinct microbial communities were detected at sites characterized either by biogenic methane seepage or thermogenic hydrocarbon seepage. A larger potential for anaerobic alkane degradation (*assA* or *bssA* and *bbsEF* genes) was detected

at the site dominated by thermogenic hydrocarbons (PC1 sediment core) containing substantial amounts of methane and higher molecular weight gaseous alkanes than in PC10 sediment samples, which contained only methane. These genes were affiliated with members of the *Desulfobacteraceae* and *Syntrophobacteraceae* families, also identified in *dsrAB* and 16S rRNA genes and transcript sequences, and are known to harbor alkane-oxidizing lineages (Bus5, *Desulfatibacillum alkenivorans*, *Desulfoglaeba alkanexedens*). However, fewer transcripts than genes involved in the degradation of alkanes and other hydrocarbons were detected in the metatranscriptome data from PC1 sediments ($\log_2$FC < 0, excepted for the *nylB* gene) (Fig. S3), suggesting marginal activity. Nevertheless, 16S rRNA and *dsrAB* transcripts from *Deltaproteobacteria* related to *Desulfatiglans anilini* and strain NaphS2, which are known to degrade aromatic compounds or polycyclic hydrocarbons (18, 52, 53), were also detected, suggesting that at least part of the sulfate-reducing bacterial community might actively degrade hydrocarbons other than methane in alkane-rich PC1 sediments, as previously suggested by measurements of hydrocarbon-degrading activity in Gulf of Mexico seep environments (7, 54).

Decreasing methane concentrations from 12 cmbsf to 2 cmbsf in PC10 sediments (2.55 μM at 10 to 12 cmbsf, 0.06 μM at 5 to 10 cmbsf and 0.04 μM at 0 to 3 cmbsf) as well as increasing δ^{13}C of methane in PC1 sediments from 10 to 12 cmbsf to the surface (–54.6‰ at 7 to 10 cmbsf, –52.8‰ at 5 to 7 cmbsf, -50.6‰ at 0 to 3 cmbsf) (Fig. 1) suggested methane oxidation in both the PC1 and PC10 cold seep sites (39). These measurements were supported by the taxonomic affiliation of 16S rRNA transcripts identified in the samples, with ANME-1 and ANME-2 archaeal lineages being predominant and active members of the microbial community, inferring that methane cycling and more particularly anaerobic methane oxidation were two of the dominant processes in these cold seep sediments of the Gulf of Mexico. These results were confirmed by the high expression level of the reverse-methanogenesis pathway as well as by the expression of the nitrogen fixation genes affiliated with ANME communities (Fig. 4; Fig. S2 and S3), as previously reported (55). Thus, despite the differences in fluid composition between seep areas PC1 and PC10, there was a considerable contribution of ANME archaea to microbial activities in these contrasting cold seep environments. Analysis of transcripts from *mcrA* and 16S rRNA genes indicated that anaerobic methanotrophic communities differed between seep sites. Seeps emitting potentially biogenic methane harbored microbial communities dominated by ANME-1b, whereas seeps producing fluids containing a complex mixture of thermogenic hydrocarbons were dominated by ANME-2 lineages. This suggests that different ANME lineages have distinct ecological requirements or metabolic capabilities, as previously suggested for other cold seep sediments (37, 56). To investigate this further, levels of gene expression in communities where either ANME-1 or ANME-2 organisms were predominant were compared.

Anaerobic oxidation of methane: ANME-1 versus ANME-2. Metagenomic and metatranscriptomic sequencing indicated that methane seep sediments in the Gulf of Mexico with relatively low methane emissions (PC10) were colonized by an active ANME-1b community (up to 64% of the 16S rRNA). All the genes needed for reverse methanogenesis were detected in these sediments. These genes and corresponding transcripts were identified on ANME-1-recruited reads; an exception was the *mer* gene, encoding an *N*5,*N*10-methylene-tetrahydromethanopterin (H_4MPT) reductase (Mer), which is an enzyme needed to oxidize methyl-H_4MPT (Fig. 4). The absence of a *mer* gene in ANME-1 lineages has been previously reported (24, 25, 57, 58). The role of Mer can be replaced by the product of *metF*, detected in our ANME-1-recruited reads, which encodes a structural analogue of Mer (23, 57). Transcripts of *metF* were expressed by ANME-1 in sediment from the PC10 core, supporting this alternative pathway. This observation is consistent with previous metatranscriptomic analysis of AOM enrichments (30). Alternatively, Mer can be replaced by the *fae-hps* gene products. These genes were detected in our ANME-1 reads and were also highly expressed ($\log_2$FC $= 2.7$

in PC10 sediments) (57, 58). The *fae-hps* gene products provide a metabolic bypass converting formaldehyde to methylene-H4MPT. However, despite the detection of the *cdhCDG* genes, encoding a methyltransferase involved in the first step of the conversion of *methyl-S*-coenzyme M to formaldehyde, genes encoding a subsequent methanol dehydrogenase were not recruited from our ANME-1 sequences or from previous ANME-1 metagenomes (58) and metaproteomes (25).

The methanogenic activities of some ANME-1 lineages have been previously suspected (13, 59). Genes for Fqo, Hdr1, and Hdr2 hydrogenase complexes were identified in ANME-1 reads, as previously observed (57), supporting a potential hydrogenotrophic methanogenesis by ANME-1. However, given the low methane concentrations measured in these sediments, the decreasing methane concentration from 12 to 2 cmbsf, and the low expression level of hydrogenase genes, the majority of ANME-1b organisms in PC10 sediment samples at the sampling time are more likely net methane consumers than producers in this system.

Known putative sulfate-reducing partners for ANME-1 (*Desulfobulbaceae*, SEEP SRB1, and SEEP SRB2) were identified. However, the 16S rRNA genes and transcripts associated with these lineages were detected at low levels (<5% of rRNA in the metatranscriptomes) compared to ANME-1 levels (32% of rRNA). The dominance of ANME-associated reads over those associated with their potential bacterial partner has been previously observed in enrichments of AOM consortia (30). Moreover, the involvement of SEEP SRB2 lineages in low-temperature AOM has been questioned (16). No *dsrAB* nor *aprA* transcripts were detected at 3 to 4 cmbsf in PC10 sediment, and expression levels at 10 to 12 cmbsf of PC10 were low (*dsrAB*, $\log_2$FC = 0.45; *aprA*, $\log_2$FC = −0.75). The expression level of *sat* genes, encoding the sulfate adenylyl-transferase, was also very low (*sat*, $\log_2$FC = −1.55; *aprA*, $\log_2$FC = −1.24), suggesting limited dissimilatory sulfate reduction activity in these sediment samples. Under these conditions, the partial sulfate depletion observed in these sediments compared to that in the PC1 sediment sample (Fig. 1) might be due to abiotic processes. Barite deposits, which form by the interaction of barium-rich seeping fluids with seawater sulfate in low flux fluid expulsion regimes, might potentially explain the sulfate depletion in the surface sediments (60). Such deposits have been observed in many cold seeps of the Gulf of Mexico (including in the Mississippi Canyon) as well as in many other cold seeps (61). Advection of low sulfate fluids, which dilutes seawater sulfate, is also possible in cold seep sediments. In addition, genes and transcripts of the assimilatory sulfate reduction pathway (CysND-CHI) were detected in PC10 sediment samples and ANME-1-recruited reads. Part of the sulfate might therefore have been slowly consumed by assimilatory sulfate reduction of the ANME-1 biomass (Fig. 5).

Gene expression profiles of the ANME-1 communities indicated very low expression levels for multiheme cytochrome *c* genes, potentially involved in extracellular electron transfer ($\log_2$FC = −1.95), suggesting that electrons from AOM were probably not transferred directly to extracellular acceptors, such as other bacteria, metal oxides, or potential extracellular organic electron acceptors (e.g., humic acids, quinones) (36). Together, these results suggest that AOM in the PC10 ANME-1b-dominated community is probably decoupled from bacterial sulfate reduction, in agreement with previous observations by FISH in other cold seep sediments (37).

It has been suggested that some ANME organisms may have a novel sulfate reduction pathway and are capable of reducing sulfate to elemental sulfur (S^0), which couples AOM to sulfate reduction in a single cell (27). There is also evidence that a number of ANME-related methanogens can reduce elemental sulfur to sulfide (62). In either case, the enzymatic mechanism remains unresolved. Genes encoding an F420-dependent sulfite reductase (Fsr) were detected in the ANME-1b-recruited reads of sample PC10 and were also expressed (Fig. 4 and Fig. S2). A sulfide detoxification function, initially identified in methanogens, was proposed for this enzyme (63). However, Fsr may catalyze parts of a novel sulfate or sulfur/polysulfide reduction pathway in ANME organisms (30). Genes and transcripts of *fsr* were also detected in PC1 hydrocarbon seep sediments dominated by members of ANME-2, suggesting potential

involvement in a detoxification process in both ANME-1 and ANME-2 lineages. However, the relative proportion of genes and transcripts was 4 times higher in ANME-1b-dominated sediments, potentially suggesting an additional role in ANME-1b metabolism.

Metatranscriptomic data highlighted that sulfide:quinone oxidoreductase-like (SQR) genes identified in the ANME-1b-recruited reads were highly expressed in PC10 sediments both at 3 to 4 cmbsf and at 10 to 12 cmbsf but not in PC1 sediments (Fig. 4 and Fig. S2) (91% of the detected SQR transcripts were homologs to the SQR sequences recruited in the ANME-1 genomic bin). SQR is a membrane-associated protein related to pyridine-nucleotide:disulfite oxidoreductase that has been characterized as a key enzyme in sulfide oxidation, producing polysulfide/elemental sulfur as the product. However, at least six types of SQR-like sequences have been defined (64), highlighting a strong heterogeneity among SQR sequences, with a functional role for half of these still unknown. Characterized SQR proteins require a sulfur oxygenase reductase (SOR) for sulfide oxidation (65); however, no SOR genes or transcripts were detected in our data set. Under anoxic conditions and in the absence of the auxiliary SOR protein, a role for SQR-like proteins in sulfide oxidation is questionable. Comparison of SQR-like amino acid sequences identified in ANME-1b sequences indicated homology (60% protein-protein similarity) with SQR-like sequences from methanogens with a sulfur-reducing capacity (*Methanolobus* sp.) (62), sulfur-reducing anaerobic *Crenarchaeota* spp. (66), and "*Candidatus* Altiarchaeales," an anaerobic archaeon from a sulfidic geyser, whose energy metabolism has not yet been established (67). All of these sulfur-reducing archaea lack a conventional sulfur reduction pathway. Therefore, we hypothesize that in elemental-sulfur/polysulfide-rich environments, SQR-like proteins might catalyze the reduction of elemental sulfur/polysulfide to H_2S. A similar hypothesis has been proposed in a deep-sea thermophile, *Thermovibrio ammonificans*, after detection of the overexpression of SQR-like genes during sulfur respiration (68). While SQR-like proteins have not been shown to reversibly catalyze sulfide oxidation/reduction yet, there are precedents for reversible enzymes. Quinone oxidoreductase (69), aldehyde oxidoreductases (70), and hydrogenases are well known to oxidize or produce hydrogen, depending on the prevailing environmental conditions. An alternative explanation for the high expression levels of ANME-1 SQR is that it operates in the oxidative direction and acts to detoxify sulfide, a role that has been proposed for a number of SQRs (71). This, however, does not reconcile the apparent lack of a metabolic pathway that would provide electron acceptors for both SQR-sulfide and methane oxidation processes in a sulfate-reducing bacterium-independent metabolism for ANME-1b in the PC10 sediment samples.

Based on these metagenomic and metatranscriptomic data, we propose a new model for bacterium-independent AOM by ANME-1b, where reverse methanogenesis might be coupled to the reduction of elemental sulfur and polysulfide (Fig. 6a), which are frequently detected in sediments of cold seep and mud volcanoes (72, 73). Even though a more extensive analysis is required to confirm the role of SQR-like proteins and F420-dependent sulfite reductase in methane oxidation by ANME-1b, thermodynamic calculations show that methane oxidation coupled to elemental sulfur/polysulfide reduction becomes exergonic ($2CH_4 + S_{9_2}^- + 4H_2O + H^+ \rightarrow 2CO_2 + 8H_2S + HS^-$; $\Delta G^{\circ\prime} = -60.87$ to -34.01 kJ/mol methane) at sulfide concentrations characteristic of methane seeps (<1 to ca. 15 mM) (74), which also correspond to sulfide concentrations that define the niche of ANME-1 (12, 37), supporting this potential metabolic pathway. These results point to new directions for future experimentations on AOM metabolism in microcosms and warrant deeper studies on SQR diversity and activity.

In contrast, in the highly active hydrocarbon seep sediment studied here (PC1), with greater fluxes of methane and other hydrocarbons, 16S rRNA, *mcrA*, and *dsrAB* gene and transcript data indicated that ANME-2c lineages (30% of the 16S rRNA) and their potential bacterial partners, the SEEP SRB1 group, were the most metabolically active members of the microbial community. This suggests that AOM by ANME-2/SEEP SRB1 consortia represented an important process in these sediments, as previously detected in other Gulf of Mexico seep sediments (6, 50).

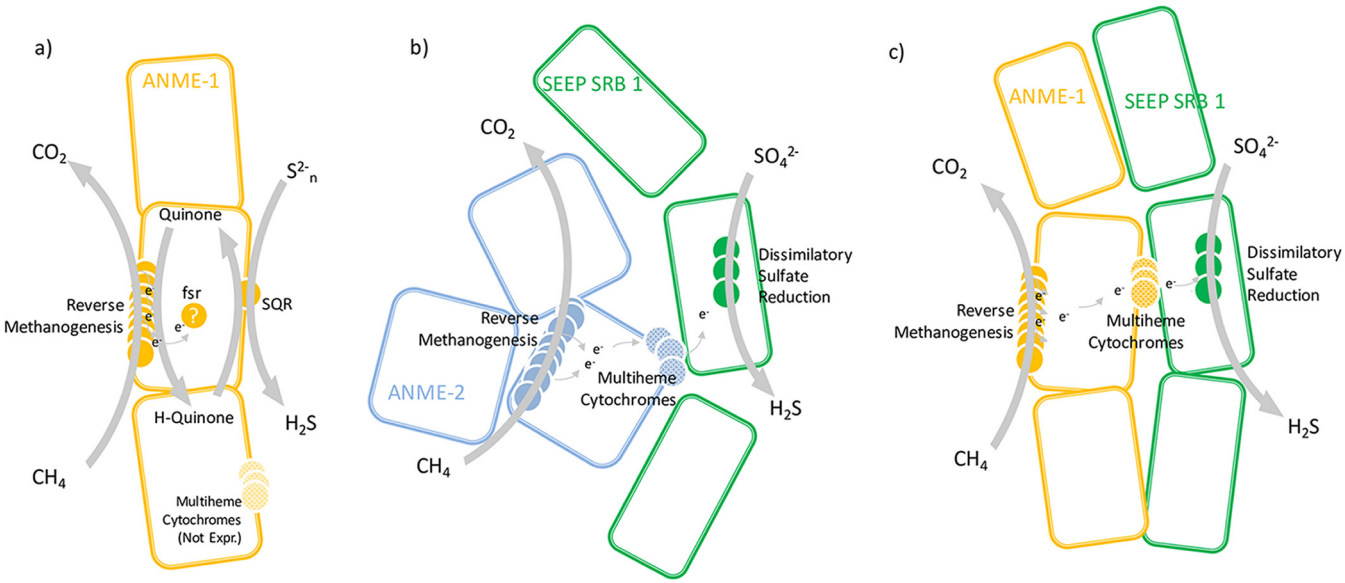

FIG 6 Model based on gene expression profiles for the anaerobic oxidation of methane pathway for ANME-1 and ANME-2 lineages detected in PC1 and PC10 sediment samples. (a) Bacterium-independent AOM by ANME-1 potentially occurring in PC10 sediment samples. Reverse methanogenesis is coupled to intracellular quinone reduction, subsequently reoxidized by polysulfide reduction through sulfide-quinone reductase (SQR). (b) AOM coupled to sulfate reduction in ANME-2/SEEP SRB1 consortia as detected in the PC1 sediment sample. Electrons from reverse methanogenesis are transferred to the sulfate-reducing SEEP SRB1 lineage through multiheme cytochromes *c*. (c) Potential metabolic pathway for AOM coupled to sulfate reduction by ANME-1/SEEP SRB1 consortia detected in the metagenomic data set of PC10 sediment samples.

In PC1 sediment samples, the expression of reverse methanogenesis pathway genes was detected at levels similar to those in the ANME-1-dominated PC10 sediments (Fig. 4). Genes of methylenetetrahydromethanopterin reductase (*mer*) were detected in PC1 metagenomic sequences but were rare in the metatranscriptomic data ($\log_2$FC = −1.42). Sequences of *mer* genes were affiliated with *Methanosarcinales* (which includes ANME-2 lineages). The *mer* gene, therefore, appeared not to be expressed during reverse methanogenesis by ANME-2c, or *mer* genes and transcripts detected belonged to minority methanogenic lineages which were also detected in PC1 sediment samples. Detection of *mer* genes in metagenomes and metatranscriptomes of single-species ANME-2a aggregates and in proteomes of ANME-2a enrichments (25), as well as in metagenomes and metatranscriptomes of nitrate-reducing ANME-2d (11), has, however, been reported. Therefore, the presence and expression of *mer* genes in anaerobic methane-oxidizing ANME-2 may be lineage dependent.

In addition to exhibiting the reverse-methanogenesis pathway, the ANME-2-rich PC1 sediment sample exhibited strong expression levels for multiheme cytochrome *c* genes ($\log_2$FC = 1.72) and genes involved in sulfate reduction (*aprAB*, *dsrAB*; $\log_2$FC = 1.05) (Fig. 3; Fig. S2). Together, these results support an earlier model for the behavior of AOM consortia where electrons from reverse methanogenesis are directly transferred to sulfate-reducing bacteria via surface multiheme cytochromes *c*, linking AOM with sulfate reduction (28, 30) (Fig. 6b). This sulfate reduction-dependent AOM is consistent with the sulfate depletion (1.71 mM sulfate) and lack of sulfite accumulation measured at 3 to 4 cmbsf in PC1 sediments, indicating canonical sulfate reduction activity, as frequently observed in highly active cold seep sites (7, 54).

Conclusions. Despite anaerobic methane oxidation being identified as the predominant potential microbial activity in sediment samples from distinct cold hydrocarbon seep environments, differences in anaerobic methanotrophic communities were detected between two seep sites. The data reported here are consistent with previous observations that ANME-1 organisms are often found as single rods-in-chain or as aggregates but without bacterial partners in deeper, more sulfidic, sediments, whereas ANME-2c/SEEP SRB1 consortia are more commonly detected in sulfate-methane transition zones and areas with highly active seepage (12, 37, 56).

Although no transcripts for multiheme cytochromes *c* were detected in PC10, genes encoding multiheme cytochromes were identified in ANME-1-recruited reads, supporting previous genomic binning (30). This might suggest that ANME-1 organisms, under different environmental conditions, might have the metabolic versatility to exchange electrons directly with a bacterial partner, as previously suggested for hydrothermal ANME-1 lineages (19, 29) (Fig. 6c). It is also not possible to exclude the potential for hydrogenotrophic methanogenesis by ANME-1b. Thus, ANME-1 organisms might adapt to changing conditions by adopting different energy-generating pathways, allowing them to occupy different ecological niches from those of other ANME lineages in marine cold seeps. Furthermore, the considerable variability of aggregate forms and architectures, as well as the complexity of the relationship between AOM consortia members previously observed (14, 16, 22, 28), suggests that other potential pathways for AOM might also exist. Our combined metagenomic and metatranscriptomic approach using intact seep sediment cores provided valuable insights toward understanding the full complexity of AOM metabolism and associated pathways.

MATERIALS AND METHODS

Sample collection. Cold seep sediment samples (15-cm-long push cores) from the Mississippi Canyon of the Gulf of Mexico were collected in October 2015 using an ROV during a sponsored seep detection and exploration cruise dedicated to oil and gas characterization. Two cold seep areas were investigated in this study (Fig. 1): (i) a slowly emitting gas seep (PC10) at 1,129 m water depth, showing sporadic bubble emission and scattered white mat-like traces at the sediment surface, and (ii) a second cold seep area (PC1), at 1,048 m of water depth, covered by orange and white microbial mats and exhibiting intense gas bubbling on the seafloor. Due to weather conditions, the number of sampling dives and coring was curtailed, and a single core per site was collected and shared between scientific teams. Sediment cores were recovered to the research vessel and immediately sectioned aseptically. Sediment layers from 1 to 3, 5 to 10, and 12 to 15 cm below the seafloor (cmbsf) were subsampled for oil and gas analysis, whereas samples from 3 to 4 and 10 to 12 cmbsf, frequently corresponding to the sulfate-to-methane transition zone and methanogenic zone, were subsampled for microbial community and pore water analysis. The PC1 sediment core was only 10 cm long, and only one sample (at 3 to 4 cmbsf) was available for microbiological analysis. Sediment sections were stored in 50-ml sterile tubes at −80°C until nucleic acid extractions were performed. From sampling to storage, the sediment samples were processed in less than 90 min. Pore water was collected from all samples following centrifugation. Anions in pore water were quantified using a Dionex ICS-2000 ion chromatograph (Thermo Scientific, Sunnyvale, CA, USA) with suppressed conductivity detection. Anions were separated on an AS11 column (Dionex) using a KOH gradient. Methane concentration and hydrocarbon composition in sediment samples were determined by gas chromatography coupled to mass spectrometry (GC-MS). Methane stable-isotope composition was determined using a gas chromatography system coupled to an isotope ratio mass spectrometer (Shimadzu, Kyoto, Japan).

Nucleic acid extraction and preparation. To ensure that a sufficient nucleic acid concentration was recovered for multiomic analyses, DNA and RNA were extracted from 2×2.5 g of sediments per sample (5 g of sediments per samples) as previously described (91) and dissolved in 200 μl of molecular-biology-grade water. For DNA-based metagenomic analyses, 50-μl samples of nucleic acid extract from each replicate were pooled and purified using a Wizard DNA cleanup kit (Promega, Madison, WI, USA). Afterwards, DNA was stored at −20°C until library preparation. A negative-control experiment of DNA and RNA extraction (procedural blanks without sediment) and purification was also carried out. The absence of contaminant was confirmed by PCR targeting the V4-V5 region of bacterial 16S rRNA genes as previously described (5). For RNA-based metatranscriptomic analyses, the remaining nucleic acids from the duplicate extractions were pooled for each sample, and RNA was purified and concentrated using a NucleoSpin RNA XS kit (Macherey-Nagel, Düren, Germany). Additional DNase treatments were carried out to remove any trace of carried-over DNA (DNase I Ambion; Life Technologies, Carlsbad, CA, USA). The absence of visible amplification of 16S rRNA genes after 35 cycles of PCR with universal primers (U515f and U919r) (75) using the RNA extracts as the template confirmed the absence of any DNA contamination. RNA was stored at −80°C and converted to cDNA within 2 days of freezing. Total RNA was used as the template for triplicate cDNA synthesis reactions using the Ovation RNA-Seq v2 system (NuGEN Technologies, San Carlos, CA, USA). To ensure sufficient cDNA concentration for library preparation, cDNA replicates were pooled before the final bead purification step and were dissolved in 20 μl of molecular-biology-grade water.

Metagenomic and metatranscriptomic library preparation, sequencing, and analysis. Metagenomic and metatranscriptomic libraries were constructed using a Nextera XT library kit (Illumina, San Diego, CA, USA) according to the manufacturer's recommendations with 1 ng of purified genomic DNA or cDNA. Tagmentation and indexing were checked using a high-sensitivity DNA chip on an Agilent Bioanalyzer 2100 (Agilent Technologies, Santa Clara, CA, USA). Libraries were normalized and diluted to 4 nM based on the average size and concentration determined from the Bioanalyzer trace. Libraries were pooled in equimolar amounts, and two pooled libraries (i.e., 2 metagenomes/transcriptomes) were sequenced per Illumina MiSeq cartridge. Metagenome/transcriptome libraries were diluted to 12.5 pM and sequenced using an Illumina MiSeq V3 kit (Illumina, San Diego, CA, USA). The sequences obtained

were barcoded and adapter trimmed on the instrument, using Illumina's MiSeq Reporter software, and downloaded from the instrument as fastq files. Data sets were quality filtered using Sickle (76), using a Q-score cutoff of >20 and a minimum read length of 60 bp. Paired-end joining was done using the join_paired_ends.py script bundled with the QIIME package (version 1.9), using default settings. Metatranscriptomic reads were assembled using Trinity (77), whereas assembly of the metagenomic reads was performed using MEGAHIT (78) and default settings. After assembly, all reads which passed quality filtering where mapped back to the assembled contigs to detect reads which were not included in the assembly using BBMap (79) and default settings. Reads which were not mapped to the assembly were concatenated with assembled contigs into a single FASTA file for upload into the IMG/M analysis pipeline (80) for gene calling and functional annotation (see Table S1 in the supplemental material). Sequence data sets were pooled and then normalized by multiple (100) rarefactions to ~130,000 KEGG orthologs (KOs) (the lowest number of KOs) for comparison of the samples. Relative abundances of genes and transcripts with predicted KOs were analyzed (Table S2). In addition, relative abundances of multiheme cytochrome *c* and *fsr* genes and transcripts were obtained by BLAST search of the reads against publicly available ANME sequences of these genes (29, 30). Positive hits with BLAST were called when the bit score was above 50 and the E value was $<e^{-15}$. The gene expression level for each sample was estimated using the $\log_2$ or $\log_{10}$ fold change ($\log_2$FC and $\log_{10}$FC, respectively) of the metatranscriptome data relative to gene counts in the corresponding metagenome.

Binning of metagenomic contigs longer than 5,000 bp was attempted using MetaBAT (81) and GroopM (82) to reconstruct ANME draft genomes. However, this approach was unsuccessful probably due to the complexity of the samples and the limited sequencing depth (83). Nevertheless, ANME-1-related sequences were recruited by BLAST search of the contigs against sequences from published fosmid libraries of ANME-1 (24, 58), and then recruited contigs were assembled with IDBA-UD (84) to generate an ANME-1 genomic bin. ANME-1-recruited reads were manually curated. Reads affiliated with bacteria (18% of the reads) were removed as potential contaminations. Completeness of the ANME-1 genomic bin was assessed using CheckM (85). A similar approach was attempted using the published ANME-2a single-aggregate genome (38) to assemble an ANME-2c metagenome from our metagenome sequence data set. However, the number of recruited contigs was limited, and assembly of an ANME-2c genomic bin was unsuccessful.

The 16S rRNA, *mcrA*, *dsrAB*, and multiheme cytochrome *c* genes and transcripts were extracted from the metagenome and metatranscriptome sequence data using vsearch against publicly available data sets for 16S rRNA (Silva release 129) (86), *mcrA* (42), *dsrAB* (43), and multiheme cytochrome *c* (29). Taxonomic affiliations of extracted genes were assigned with BLAST against their respective database using QIIME 1.9.1 (87). For phylogenetic tree construction, full-length *dsrAB* and *mcrA* genes were reconstructed from metagenomic and metatranscriptomic reads using Xander (88), followed by sequence alignment using MAFFT (89). Phylogenetic trees were estimated using the neighbor-joining method, with distances calculated with Kimura's two-parameter model using MEGA4 (90). The robustness of the inferred topology was tested by bootstrap resampling (1,000 replicates).

Accession number(s). Metagenomes and metatranscriptomes are available in the IMG/M database under the following accession numbers: 3300008741, 3300009865, 3300009874, 3300008468, 3300008633, and 3300008340.

SUPPLEMENTAL MATERIAL

Supplemental material for this article may be found at https://doi.org/10.1128/mSystems.00091-18.

FIG S1, TIF file, 1 MB.

FIG S2, TIF file, 1 MB.

FIG S3, TIF file, 0.4 MB.

TABLE S1, XLSX file, 0.01 MB.

TABLE S2, XLSX file, 0.3 MB.

ACKNOWLEDGMENTS

This work was funded by Shell Global Solutions International BV and the Natural Environment Research Council OILSPORE project (NE/J024325/1) and was also supported by the U.S. Department of Energy (DOE) Joint Genome Institute, a DOE Office of Science User Facility, under contract no. DE-AC02-05CH11231. The authors declare no conflict of interest.

REFERENCES

1. Jorgensen BB, Boetius A. 2007. Feast and famine—microbial life in the deep-sea bed. Nat Rev Microbiol 5:770–781. https://doi.org/10.1038/nrmicro1745.
2. Cruaud P, Vigneron A, Pignet P, Caprais J-C, Lesongeur F, Toffin L, Godfroy A, Cambon-Bonavita M-A. 2015. Microbial communities associated with benthic faunal assemblages at cold seep sediments of the Sonora Margin, Guaymas Basin. Front Mar Sci 2:53. https://doi.org/10.3389/fmars.2015.00053.
3. Niemann H, Losekann T, de Beer D, Elvert M, Nadalig T, Knittel K, Amann R, Sauter EJ, Schluter M, Klages M, Foucher JP, Boetius A. 2006. Novel microbial communities of the Haakon Mosby mud volcano and their role as a methane sink. Nature 443:854–858. https://doi.org/10.1038/nature05227.

4. Teske A, Sorensen KB. 2008. Uncultured archaea in deep marine subsurface sediments: have we caught them all? ISME J 2:3–18. https://doi.org/10.1038/ismej.2007.90.
5. Vigneron A, Alsop EB, Cruaud P, Philibert G, King B, Baksmaty L, Lavallée D, Lomans BP, Kyrpides NC, Head IM, Tsesmetzis N. 2017. Comparative metagenomics of hydrocarbon and methane seeps of the Gulf of Mexico. Sci Rep 7:16015. https://doi.org/10.1038/s41598-017-16375-5.
6. Orcutt BN, Joye SB, Kleindienst S, Knittel K, Ramette A, Reitz A, Samarkin V, Treude T, Boetius A. 2010. Impact of natural oil and higher hydrocarbons on microbial diversity, distribution, and activity in Gulf of Mexico cold-seep sediments. Gulf Mex Cold Seeps 57:2008–2021. https://doi.org/10.1016/j.dsr2.2010.05.014.
7. Joye SB, Bowles MW, Samarkin VA, Hunter KS, Niemann H. 2010. Biogeochemical signatures and microbial activity of different cold-seep habitats along the Gulf of Mexico deep slope. Gulf Mex Cold Seeps 57:1990–2001. https://doi.org/10.1016/j.dsr2.2010.06.001.
8. Ruff SE, Biddle JF, Teske AP, Knittel K, Boetius A, Ramette A. 2015. Global dispersion and local diversification of the methane seep microbiome. Proc Natl Acad Sci U S A 112:4015–4020. https://doi.org/10.1073/pnas.1421865112.
9. Knittel K, Boetius A. 2009. Anaerobic oxidation of methane: progress with an unknown process. Annu Rev Microbiol 63:311–334. https://doi.org/10.1146/annurev.micro.61.080706.093130.
10. Boetius A, Ravenschlag K, Schubert CJ, Rickert D, Widdel F, Gieseke A, Amann R, Jorgensen BB, Witte U, Pfannkuche O. 2000. A marine microbial consortium apparently mediating anaerobic oxidation of methane. Nature 407:623–626. https://doi.org/10.1038/35036572.
11. Haroon MF, Hu S, Shi Y, Imelfort M, Keller J, Hugenholtz P, Yuan Z, Tyson GW. 2013. Anaerobic oxidation of methane coupled to nitrate reduction in a novel archaeal lineage. Nature 500:567–570. https://doi.org/10.1038/nature12375.
12. Biddle JF, Cardman Z, Mendlovitz H, Albert DB, Lloyd KG, Boetius A, Teske A. 2012. Anaerobic oxidation of methane at different temperature regimes in Guaymas Basin hydrothermal sediments. ISME J 6:1018–1031. https://doi.org/10.1038/ismej.2011.164.
13. Beulig F, Røy H, McGlynn SE, Jørgensen BB. 2019. Cryptic CH4 cycling in the sulfate–methane transition of marine sediments apparently mediated by ANME-1 archaea. ISME J 13:250–262. https://doi.org/10.1038/s41396-018-0273-z.
14. Schreiber L, Holler T, Knittel K, Meyerdierks A, Amann R. 2010. Identification of the dominant sulfate-reducing bacterial partner of anaerobic methanotrophs of the ANME-2 clade. Environ Microbiol 12:2327–2340. https://doi.org/10.1111/j.1462-2920.2010.02275.x.
15. Pernthaler A, Dekas AE, Brown CT, Goffredi SK, Embaye T, Orphan VJ. 2008. Diverse syntrophic partnerships from deep-sea methane vents revealed by direct cell capture and metagenomics. Proc Natl Acad Sci U S A 105:7052–7057. https://doi.org/10.1073/pnas.0711303105.
16. Vigneron A, Cruaud P, Pignet P, Caprais J-C, Gayet N, Cambon-Bonavita M-A, Godfroy A, Toffin L. 2014. Bacterial communities and syntrophic associations involved in anaerobic oxidation of methane process of the Sonora Margin cold seeps, Guaymas Basin. Environ Microbiol 16:2777–2790. https://doi.org/10.1111/1462-2920.12324.
17. Lösekann T, Knittel K, Nadalig T, Fuchs B, Niemann H, Boetius A, Amann R. 2007. Diversity and abundance of aerobic and anaerobic methane oxidizers at the Haakon Mosby Mud Volcano, Barents Sea. Appl Environ Microbiol 73:3348–3362. https://doi.org/10.1128/AEM.00016-07.
18. Kleindienst S, Ramette A, Amann R, Knittel K. 2012. Distribution and in situ abundance of sulfate-reducing bacteria in diverse marine hydrocarbon seep sediments. Environ Microbiol 14:2689–2710. https://doi.org/10.1111/j.1462-2920.2012.02832.x.
19. Wegener G, Krukenberg V, Ruff SE, Kellermann MY, Knittel K. 2016. Metabolic capabilities of microorganisms involved in and associated with the anaerobic oxidation of methane. Front Microbiol 7:46. https://doi.org/10.3389/fmicb.2016.00046.
20. Holler T, Widdel F, Knittel K, Amann R, Kellermann MY, Hinrichs K-U, Teske A, Boetius A, Wegener G. 2011. Thermophilic anaerobic oxidation of methane by marine microbial consortia. ISME J 5:1946–1956. https://doi.org/10.1038/ismej.2011.77.
21. Krukenberg V, Harding K, Richter M, Glöckner FO, Gruber-Vodicka HR, Adam B, Berg JS, Knittel K, Tegetmeyer HE, Boetius A, Wegener G. 2016. Candidatus Desulfofervidus auxilii, a hydrogenotrophic sulfate-reducing bacterium involved in the thermophilic anaerobic oxidation of methane. Environ Microbiol 18:3073–3091. https://doi.org/10.1111/1462-2920.13283.
22. Hatzenpichler R, Connon SA, Goudeau D, Malmstrom RR, Woyke T, Orphan VJ. 2016. Visualizing in situ translational activity for identifying and sorting slow-growing archaeal–bacterial consortia. Proc Natl Acad Sci U S A 113:E4069–E4078. https://doi.org/10.1073/pnas.1603757113.
23. Timmers PHA, Welte CU, Koehorst JJ, Plugge CM, Jetten MSM, Stams AJM. 2017. Reverse methanogenesis and respiration in methanotrophic archaea. Archaea 2017:1654237. https://doi.org/10.1155/2017/1654237.
24. Hallam SJ, Putnam N, Preston CM, Detter JC, Rokhsar D, Richardson PM, DeLong EF. 2004. Reverse methanogenesis: testing the hypothesis with environmental genomics. Science 305:1457. https://doi.org/10.1126/science.1100025.
25. Marlow JJ, Skennerton CT, Li Z, Chourey K, Hettich RL, Pan C, Orphan VJ. 2016. Proteomic stable isotope probing reveals biosynthesis dynamics of slow growing methane based microbial communities. Front Microbiol 7:563. https://doi.org/10.3389/fmicb.2016.00563.
26. Stams AJM, Plugge CM. 2009. Electron transfer in syntrophic communities of anaerobic bacteria and archaea. Nat Rev Microbiol 7:568–577. https://doi.org/10.1038/nrmicro2166.
27. Milucka J, Ferdelman TG, Polerecky L, Franzke D, Wegener G, Schmid M, Lieberwirth I, Wagner M, Widdel F, Kuypers MMM. 2012. Zero-valent sulphur is a key intermediate in marine methane oxidation. Nature 491:541–546. https://doi.org/10.1038/nature11656.
28. McGlynn SE, Chadwick GL, Kempes CP, Orphan VJ. 2015. Single cell activity reveals direct electron transfer in methanotrophic consortia. Nature 526:531–535. https://doi.org/10.1038/nature15512.
29. Wegener G, Krukenberg V, Riedel D, Tegetmeyer HE, Boetius A. 2015. Intercellular wiring enables electron transfer between methanotrophic archaea and bacteria. Nature 526:587–590. https://doi.org/10.1038/nature15733.
30. Krukenberg V, Riedel D, Gruber-Vodicka HR, Buttigieg PL, Tegetmeyer HE, Boetius A, Wegener G. 2018. Gene expression and ultrastructure of meso- and thermophilic methanotrophic consortia: interspecies interaction within AOM consortia. Environ Microbiol 20:1651–1666. https://doi.org/10.1111/1462-2920.14077.
31. Skennerton CT, Chourey K, Iyer R, Hettich RL, Tyson GW, Orphan VJ. 2017. Methane-fueled syntrophy through extracellular electron transfer: uncovering the genomic traits conserved within diverse bacterial partners of anaerobic methanotrophic archaea. mBio 8:e00530-17. https://doi.org/10.1128/mBio.00530-17.
32. Raghoebarsing AA, Pol A, van de Pas-Schoonen KT, Smolders AJP, Ettwig KF, Rijpstra WIC, Schouten S, Damsté JSS, Op den Camp HJM, Jetten MSM, Strous M. 2006. A microbial consortium couples anaerobic methane oxidation to denitrification. Nature 440:918–921. https://doi.org/10.1038/nature04617.
33. Ettwig KF, Zhu B, Speth D, Keltjens JT, Jetten MSM, Kartal B. 2016. Archaea catalyze iron-dependent anaerobic oxidation of methane. Proc Natl Acad Sci U S A 113:12792–12796. https://doi.org/10.1073/pnas.1609534113.
34. Beal EJ, House CH, Orphan VJ. 2009. Manganese- and iron-dependent marine methane oxidation. Science 325:184. https://doi.org/10.1126/science.1169984.
35. Cai C, Leu AO, Xie G-J, Guo J, Feng Y, Zhao J-X, Tyson GW, Yuan Z, Hu S. 2018. A methanotrophic archaeon couples anaerobic oxidation of methane to Fe(III) reduction. ISME J 12:1929–1939. https://doi.org/10.1038/s41396-018-0109-x.
36. Scheller S, Yu H, Chadwick GL, McGlynn SE, Orphan VJ. 2016. Artificial electron acceptors decouple archaeal methane oxidation from sulfate reduction. Science 351:703. https://doi.org/10.1126/science.aad7154.
37. Vigneron A, Cruaud P, Pignet P, Caprais J-C, Cambon-Bonavita M-A, Godfroy A, Toffin L. 2013. Archaeal and anaerobic methane oxidizer communities in the Sonora Margin cold seeps, Guaymas Basin (Gulf of California). ISME J 7:1595–1608. https://doi.org/10.1038/ismej.2013.18.
38. Wang F-P, Zhang Y, Chen Y, He Y, Qi J, Hinrichs K-U, Zhang X-X, Xiao X, Boon N. 2014. Methanotrophic archaea possessing diverging methane-oxidizing and electron-transporting pathways. ISME J 8:1069–1078. https://doi.org/10.1038/ismej.2013.212.
39. Whiticar MJ. 1999. Carbon and hydrogen isotope systematics of bacterial formation and oxidation of methane. Chem Geol 161:291–314. https://doi.org/10.1016/S0009-2541(99)00092-3.
40. Wagner M, Rath G, Amann R, Koops H-P, Schleifer K-H. 1995. In situ identification of ammonia-oxidizing bacteria. Syst Appl Microbiol 18:251–264. https://doi.org/10.1016/S0723-2020(11)80396-6.
41. Blazewicz SJ, Barnard RL, Daly RA, Firestone MK. 2013. Evaluating rRNA as an indicator of microbial activity in environmental communities:

limitations and uses. ISME J 7:2061. https://doi.org/10.1038/ismej.2013.102.
42. Vigneron A, Bishop A, Alsop E, Hull K, Rhodes I, Hendricks R, Head I, Tsesmetzis N. 2017. Microbial and isotopic evidence for methane cycling in hydrocarbon-containing groundwater from the Pennsylvania region. Front Microbiol 8:593. https://doi.org/10.3389/fmicb.2017.00593.
43. Muller AL, Kjeldsen KU, Rattei T, Pester M, Loy A. 2015. Phylogenetic and environmental diversity of DsrAB-type dissimilatory (bi)sulfite reductases. ISME J 9:1152–1165. https://doi.org/10.1038/ismej.2014.208.
44. Carvalhais LC, Dennis PG, Tyson GW, Schenk PM. 2012. Application of metatranscriptomics to soil environments. J Microbiol Methods 91:246–251. https://doi.org/10.1016/j.mimet.2012.08.011.
45. Ishii S, Suzuki S, Tenney A, Nealson KH, Bretschger O. 2018. Comparative metatranscriptomics reveals extracellular electron transfer pathways conferring microbial adaptivity to surface redox potential changes. ISME J 12:2844–2863. https://doi.org/10.1038/s41396-018-0238-2.
46. Reid T, Chaganti SR, Droppo IG, Weisener CG. 2018. Novel insights into freshwater hydrocarbon-rich sediments using metatranscriptomics: opening the black box. Water Res 136:1–11. https://doi.org/10.1016/j.watres.2018.02.039.
47. Woodcroft BJ, Singleton CM, Boyd JA, Evans PN, Emerson JB, Zayed AAF, Hoelzle RD, Lamberton TO, McCalley CK, Hodgkins SB, Wilson RM, Purvine SO, Nicora CD, Li C, Frolking S, Chanton JP, Crill PM, Saleska SR, Rich VI, Tyson GW. 2018. Genome-centric view of carbon processing in thawing permafrost. Nature 560:49–54. https://doi.org/10.1038/s41586-018-0338-1.
48. Mills HJ, Martinez RJ, Story S, Sobecky PA. 2004. Identification of members of the metabolically active microbial populations associated with Beggiatoa species mat communities from Gulf of Mexico cold-seep sediments. Appl Environ Microbiol 70:5447–5458. https://doi.org/10.1128/AEM.70.9.5447-5458.2004.
49. Orphan VJ, House CH, Hinrichs K-U, McKeegan KD, DeLong EF. 2002. Multiple archaeal groups mediate methane oxidation in anoxic cold seep sediments. Proc Natl Acad Sci U S A 99:7663–7668. https://doi.org/10.1073/pnas.072210299.
50. Lloyd KG, Albert DB, Biddle JF, Chanton JP, Pizarro O, Teske A. 2010. Spatial structure and activity of sedimentary microbial communities underlying a Beggiatoa spp. mat in a Gulf of Mexico hydrocarbon seep. PLoS One 5:e8738. https://doi.org/10.1371/journal.pone.0008738.
51. Dekas AE, Connon SA, Chadwick GL, Trembath-Reichert E, Orphan VJ. 2016. Activity and interactions of methane seep microorganisms assessed by parallel transcription and FISH-NanoSIMS analyses. ISME J 10:678–692. https://doi.org/10.1038/ismej.2015.145.
52. Galushko A, Minz D, Schink B, Widdel F. 1999. Anaerobic degradation of naphthalene by a pure culture of a novel type of marine sulphate-reducing bacterium. Environ Microbiol 1:415–420. https://doi.org/10.1046/j.1462-2920.1999.00051.x.
53. Widdel F, Knittel K, Galushko A. 2010. Anaerobic hydrocarbon-degrading microorganisms: an overview, p 1997–2021. *In* Timmis KN (ed), Handbook of hydrocarbon and lipid microbiology. Springer, Berlin, Germany.
54. Orcutt B, Boetius A, Elvert M, Samarkin V, Joye SB. 2005. Molecular biogeochemistry of sulfate reduction, methanogenesis and the anaerobic oxidation of methane at Gulf of Mexico cold seeps. Geochim Cosmochim Acta 69:4267–4281. https://doi.org/10.1016/j.gca.2005.04.012.
55. Dekas AE, Poretsky RS, Orphan VJ. 2009. Deep-sea archaea fix and share nitrogen in methane-consuming microbial consortia. Science 326:422. https://doi.org/10.1126/science.1178223.
56. Yanagawa K, Sunamura M, Lever MA, Morono Y, Hiruta A, Ishizaki O, Matsumoto R, Urabe T, Inagaki F. 2011. Niche separation of methanotrophic archaea (ANME-1 and -2) in methane-seep sediments of the eastern Japan Sea offshore Joetsu. Geomicrobiol J 28:118–129. https://doi.org/10.1080/01490451003709334.
57. Stokke R, Roalkvam I, Lanzen A, Haflidason H, Steen IH. 2012. Integrated metagenomic and metaproteomic analyses of an ANME-1-dominated community in marine cold seep sediments. Environ Microbiol 14:1333–1346. https://doi.org/10.1111/j.1462-2920.2012.02716.x.
58. Meyerdierks A, Kube M, Kostadinov I, Teeling H, Glöckner FO, Reinhardt R, Amann R. 2010. Metagenome and mRNA expression analyses of anaerobic methanotrophic archaea of the ANME-1 group. Environ Microbiol 12:422–439. https://doi.org/10.1111/j.1462-2920.2009.02083.x.
59. Lloyd KG, Alperin MJ, Teske A. 2011. Environmental evidence for net methane production and oxidation in putative ANaerobic MEthanotrophic (ANME) archaea. Environ Microbiol 13:2548–2564. https://doi.org/10.1111/j.1462-2920.2011.02526.x.
60. Aloisi G, Wallmann K, Bollwerk SM, Derkachev A, Bohrmann G, Suess E. 2004. The effect of dissolved barium on biogeochemical processes at cold seeps. Geochim Cosmochim Acta 68:1735–1748. https://doi.org/10.1016/j.gca.2003.10.010.
61. Feng D, Roberts HH. 2011. Geochemical characteristics of the barite deposits at cold seeps from the northern Gulf of Mexico continental slope. Earth Planet Sci Lett 309:89–99. https://doi.org/10.1016/j.epsl.2011.06.01.
62. Stetter KO, Gaag G. 1983. Reduction of molecular sulphur by methanogenic bacteria. Nature 305:309–311. https://doi.org/10.1038/305309a0.
63. Johnson EF, Mukhopadhyay B. 2008. Coenzyme F420-dependent sulfite reductase-enabled sulfite detoxification and use of sulfite as a sole sulfur source by Methanococcus maripaludis. Appl Environ Microbiol 74:3591–3595. https://doi.org/10.1128/AEM.00098-08.
64. Marcia M, Ermler U, Peng G, Michel H. 2010. A new structure-based classification of sulfide:quinone oxidoreductases. Proteins 78:1073–1083. https://doi.org/10.1002/prot.22665.
65. Dahl C, Schulte A, Stockdreher Y, Hong C, Grimm F, Sander J, Kim R, Kim S-H, Shin DH. 2008. Structural and molecular genetic insight into a widespread sulfur oxidation pathway. J Mol Biol 384:1287–1300. https://doi.org/10.1016/j.jmb.2008.10.016.
66. Itoh T, Suzuki K, Nakase T. 2002. Vulcanisaeta distributa gen. nov., sp. nov., and Vulcanisaeta souniana sp. nov., novel hyperthermophilic, rod-shaped crenarchaeotes isolated from hot springs in Japan. Int J Syst Evol Microbiol 52:1097–1104. https://doi.org/10.1099/00207713-52-4-1097.
67. Probst AJ, Weinmaier T, Raymann K, Perras A, Emerson JB, Rattei T, Wanner G, Klingl A, Berg IA, Yoshinaga M, Viehweger B, Hinrichs K-U, Thomas BC, Meck S, Auerbach AK, Heise M, Schintlmeister A, Schmid M, Wagner M, Gribaldo S, Banfield JF, Moissl-Eichinger C. 2014. Biology of a widespread uncultivated archaeon that contributes to carbon fixation in the subsurface. Nat Commun 5:5497. https://doi.org/10.1038/ncomms6497.
68. Jelen B, Giovannelli D, Falkowski PG, Vetriani C. 2018. Elemental sulfur reduction in the deep-sea vent thermophile, Thermovibrio ammonificans. Environ Microbiol 20:2301–2316. https://doi.org/10.1111/1462-2920.14280.
69. Brandt U. 2006. Energy converting NADH: quinone oxidoreductase (complex I). Annu Rev Biochem 75:69–92. https://doi.org/10.1146/annurev.biochem.75.103004.142539.
70. Huber C, Caldeira J, Jongejan JA, Simon H. 1994. Further characterization of two different, reversible aldehyde oxidoreductases from Clostridium formicoaceticum, one containing tungsten and the other molybdenum. Arch Microbiol 162:303–309. https://doi.org/10.1007/BF00263776.
71. Marcia M, Ermler U, Peng G, Michel H. 2010. A new structure-based classification of sulfide:quinone oxidoreductases. Proteins Struct Funct Bioinforma 78:1073–1083. https://doi.org/10.1002/prot.22665.
72. Zhang X, Du Z, Zheng R, Luan Z, Qi F, Cheng K, Wang B, Ye W, Liu X, Lian C, Chen C, Guo J, Li Y, Yan J. 2017. Development of a new deep-sea hybrid Raman insertion probe and its application to the geochemistry of hydrothermal vent and cold seep fluids. Deep Sea Res Part 1 Oceanogr Res Pap 123:1–12. https://doi.org/10.1016/j.dsr.2017.02.005.
73. Findlay AJ. 2016. Microbial impact on polysulfide dynamics in the environment. FEMS Microbiol Lett 363:fnw103. https://doi.org/10.1093/femsle/fnw103.
74. Boetius A, Suess E. 2004. Hydrate Ridge: a natural laboratory for the study of microbial life fueled by methane from near-surface gas hydrates. Chem Geol 205:291–310. https://doi.org/10.1016/j.chemgeo.2003.12.034.
75. Klindworth A, Pruesse E, Schweer T, Peplies J, Quast C, Horn M, Glöckner FO. 2013. Evaluation of general 16S ribosomal RNA gene PCR primers for classical and next-generation sequencing-based diversity studies. Nucleic Acids Res 41:e1. https://doi.org/10.1093/nar/gks808.
76. Joshi N, Fass J. 2011. Sickle: a sliding-window, adaptive, quality-based trimming tool for FastQ files. Version 1.33. Available at https://github.com/najoshi/sickle.
77. Grabherr MG, Haas BJ, Yassour M, Levin JZ, Thompson DA, Amit I, Adiconis X, Fan L, Raychowdhury R, Zeng Q, Chen Z, Mauceli E, Hacohen N, Gnirke A, Rhind N, di Palma F, Birren BW, Nusbaum C, Lindblad-Toh K, Friedman N, Regev A. 2011. Full-length transcriptome assembly from RNA-Seq data without a reference genome. Nat Biotechnol 29:644–652. https://doi.org/10.1038/nbt.1883.
78. Li D, Liu C-M, Luo R, Sadakane K, Lam T-W. 2015. MEGAHIT: an ultra-fast single-node solution for large and complex metagenomics assembly via

succinct de Bruijn graph. Bioinformatics 31:1674–1676. https://doi.org/10.1093/bioinformatics/btv033.
79. Bushnell B. 2014. BBMap: a fast, accurate, splice-aware aligner. Ernest Orlando Lawrence Berkeley National Laboratory, Berkeley, CA.
80. Markowitz VM, Mavromatis K, Ivanova NN, Chen I-MA, Chu K, Kyrpides NC. 2009. IMG ER: a system for microbial genome annotation expert review and curation. Bioinformatics 25:2271–2278. https://doi.org/10.1093/bioinformatics/btp393.
81. Kang DD, Froula J, Egan R, Wang Z. 2015. MetaBAT, an efficient tool for accurately reconstructing single genomes from complex microbial communities. PeerJ 3:e1165. https://doi.org/10.7717/peerj.1165.
82. Imelfort M, Parks D, Woodcroft BJ, Dennis P, Hugenholtz P, Tyson GW. 2014. GroopM: an automated tool for the recovery of population genomes from related metagenomes. PeerJ 2:e603. https://doi.org/10.7717/peerj.603.
83. Vollmers J, Wiegand S, Kaster A-K. 2017. Comparing and evaluating metagenome assembly tools from a microbiologist's perspective—not only size matters! PLoS One 12:e0169662. https://doi.org/10.1371/journal.pone.0169662.
84. Peng Y, Leung HCM, Yiu SM, Chin FYL. 2012. IDBA-UD: a de novo assembler for single-cell and metagenomic sequencing data with highly uneven depth. Bioinformatics 28:1420–1428. https://doi.org/10.1093/bioinformatics/bts174.
85. Parks DH, Imelfort M, Skennerton CT, Hugenholtz P, Tyson GW. 2015. CheckM: assessing the quality of microbial genomes recovered from isolates, single cells, and metagenomes. Genome Res 25:1043–1055. https://doi.org/10.1101/gr.186072.114.
86. Pruesse E, Quast C, Knittel K, Fuchs BM, Ludwig W, Peplies J, Glöckner FO. 2007. SILVA: a comprehensive online resource for quality checked and aligned ribosomal RNA sequence data compatible with ARB. Nucleic Acids Res 35:7188–7196. https://doi.org/10.1093/nar/gkm864.
87. Caporaso JG, Kuczynski J, Stombaugh J, Bittinger K, Bushman FD, Costello EK, Fierer N, Pena AG, Goodrich JK, Gordon JI, Huttley GA, Kelley ST, Knights D, Koenig JE, Ley RE, Lozupone CA, McDonald D, Muegge BD, Pirrung M, Reeder J, Sevinsky JR, Turnbaugh PJ, Walters WA, Widmann J, Yatsunenko T, Zaneveld J, Knight R. 2010. QIIME allows analysis of high-throughput community sequencing data. Nat Methods 7:335–336. https://doi.org/10.1038/nmeth.f.303.
88. Wang Q, Fish JA, Gilman M, Sun Y, Brown CT, Tiedje JM, Cole JR. 2015. Xander: employing a novel method for efficient gene-targeted metagenomic assembly. Microbiome 3:32. https://doi.org/10.1186/s40168-015-0093-6.
89. Katoh K, Misawa K, Kuma K, Miyata T. 2002. MAFFT: a novel method for rapid multiple sequence alignment based on fast Fourier transform. Nucleic Acids Res 30:3059–3066. https://doi.org/10.1093/nar/gkf436.
90. Tamura K, Dudley J, Nei M, Kumar S. 2007. MEGA4: Molecular Evolutionary Genetics Analysis (MEGA) software version 4.0. Mol Biol Evol 24:1596. https://doi.org/10.1093/molbev/msm092.
91. Zhou J, Bruns MA, Tiedje JM. 1996. DNA recovery from soils of diverse composition. Appl Environ Microbiol 62:316–322.